Research Article

Development of dual enzyme responsive molecular AND logic gate

Sündüs ERBAŞ ÇAKMAK[1,2],*

[1]Department of Molecular Biology and Genetics, Konya Food and Agriculture University, Konya, Turkey
[2]Biotechnology Graduate Program, Konya Food and Agriculture University, Konya, Turkey

Abstract: Molecular logic gates are information processing devices that can respond to environmental signals and produce a readable output in response through Boolean logic operations. Molecules with these properties have been used to build smart sensors and therapeutic agents. In this work, dual enzyme-responsive molecular AND logic gate is developed with the intention to discriminate various combinations of enzyme level and/or activity. A resorufin-based sensor is substituted with self-immolative tyrosinase recognition site, 3-hydroxy benzyl group. The Hydroxyl group is protected with acetyl moiety which decreases the affinity of the enzyme. When both tyrosinase and esterase are present in the solution, the acetyl group is removed by the latter enzyme, allowing the former to recognise the ligand. Oxidation of the ligand by tyrosinase triggers self-immolative cleavage of the substitution, leading to almost 70 fold enhancement in fluorescence. When single enzyme is applied, there is no significant change in the emission intensity overall, an AND logic gate is constructed. Selectivity and Michaelis-Menten kinetics of the sensor is analysed. Smart molecular probes can contribute to the research on the development of biosensors that can discriminate diseases having characteristic combinations of enzyme activities.

Key words: Molecular logic gates, enzyme sensor, fluorescence, resorufin

1. Introduction

Molecules can be functionalized rationally to be responsive to their environments. Various acivatable therapeutics, molecular sensors that produce a readable output signal in the presence of analyte have been widely studied in the literature [1,2]. In the last decade, significant progress in the design of such systems has been taken. Molecules are further modified to have additional features, multianalyte responsiveness. These findings lead to the discovery of a new concept, molecular logic gates. Logic operations are well-defined mathematical operations where inputs and outputs are characterised by certain rules [3]. Analyte level or response output level beyond a certain threshold are accepted as '1' and the absence of them are given the value of '0'. Similar to computer algorithms, this digitalized data is used for logic operations. A potential chemical and biological application of these operations with molecular devices is started to be discussed after the introduction of the molecular logic gate by de Silva et. al. [4]. In this pioneering work, the molecule can detect the inputs (acid and sodium ion), and produces an output in the form of fluorescence. Later, the idea is used to develop many different advanced logic gates such as DEMUX, FLIP-FLOP logics as well as integrated logic gates [5]. Some of these logic gates are shown to have potential applications as smart therapeutics or biosensors [6–20]. Recently, our research group designed a molecular keypad lock to show that information processing devices can have selective therapeutic activity in drug-resistant cancer cells, through a sequential analyte responsiveness and molecular encryption [6]. Theranostic approaches, by which a combinatorial imaging and therapeutic effect can be achieved, is also shown to be possible with advanced molecular logic gate operations [7,8].

Enzymes are biological catalysts whose levels and activities are strictly regulated. Depending on the needs of the cells, extracellular and/or intracellular signals, enzymes are produced, degraded, activated or deactivated. Diseases, including cancer, are usually characterised by abnormal level or activity of a group of enzymes [21]. For that, elevated level of enzymes is considered as a disease marker and various molecular sensors are developed to detect enzyme levels [22,23]. Although diseases can be monitored by following the enzyme level, tissue expression of enzymes may also differ in a healthy organism [24]. The enzyme of interest may also be overexpressed in a different tissue under normal conditions. This may lead to misinterpretation of the data. This constitutes a major problem with single enzyme sensing for diagnostic

567

applications, and a direct correlation between enzyme level and the disease status cannot be achieved. For that, more than one enzyme (or analyte) can be monitored to selectively discriminate healthy tissue from the diseased one. Molecular AND logic operations are suitable devices to have this discrimination. When truth tables of this operation are analysed, these devices only produce an output in the presence of all inputs. In other words, a diagnostic signal is produced when all of the disease parameters are sufficiently high. Previously various dual enzyme sensing probes are reported [25–30]. To the best of our knowledge, there is no fluorescent small-molecule probe dual responsive to tyrosinase and esterase enzymes, which is aimed in this work.

In the research, an esterase and tyrosinase responsive fluorescent probe 2 is designed as shown in Scheme 1. Resorufin dye is functionalised with tyrosinase enzyme ligand, 3-hydroxy benzyl moiety. This group is known to be oxidized by the enzyme to produce, 3,4-dihydroxy benzyl derivative [31–34]. This self-immolative linker detaches from the parent fluorophore spontaneously by rapid 1,6-elimination reaction, producing fluorescent resorufin (Scheme 1). 3-Hydroxy benzyl recognition unit is preferred because of its stability towards other reactive oxygen species [31]. In this work, phenolic OH is protected with the acyl group to avoid tyrosinase recognition. Upon removal of the acyl group by an esterase, tyrosinase can recognise and oxidise the probe [6]. Therefore, with the action of two enzymes, a fluorescence signal is expected to be produced. Dual enzyme responsiveness is intended to enable accurate discrimination of various phenotypes of diseases for future applications. Tyrosinase enzyme is an oxidative enzyme either catalyses second oxidation of phenolic compounds or produces quinones from diphenols [35]. It is involved in L-DOPA and melanin biosynthesis. Several diseases including Parkinson's disease and melanoma cancers are reported to show an abnormal level of this enzyme [36, 37]. Esterase enzymes are hydrolytic enzymes responsible for the cleavage of ester bonds. They are known to have roles in drug detoxification and are associated with drug resistance [38]. Therefore, designing a probe responsive to both of these enzymes would enable discrimination of melanoma cancers or Parkinson's disease that are resistant to traditional chemotherapies. This strategy can be further extended to display response in the presence of various combinations of other enzyme disease markers.

Resorufin is a small fluorescent molecule that has been previously used for many biosensing applications [39, 40]. Functionalization of the OH moiety is known to reduce fluorescence. Once the substituent is removed by the analyte of interest, fluorescence can be reestablished. This TURN-ON fluorescent sensing approach was used to prepare probes for several analytes including enzymes [34, 39–43]. Recently, tyrosinase responsive probe based on resorufin skeleton is also reported with efficient and selective response to this enzyme [34]. In this work, dual responsiveness is generated by hiding the tyrosinase recognition site with acyl group. Acyl groups are previously reported to be removed by the esterase enzymes [6].

2. Experimental
General information about the materials, equipment, additional experimental and characterization data are given as supplementary information.

2.1. Synthesis

2.1.1. 3-(bromomethyl)phenyl acetate (1)
3-Hydroxybenzyl bromide (94 mg, 0.50 mmol) was dissolved in 10 mL dichloromethane. Triethylamine (0.14 mL, 1 mmol) and acetyl chloride (72 μL, 1 mmol) were added (Scheme 2). The reaction was stirred for 16 h at room temperature and then extracted with dichloromethane and water. The organic layer is collected and dried using sodium sulfate. The solution
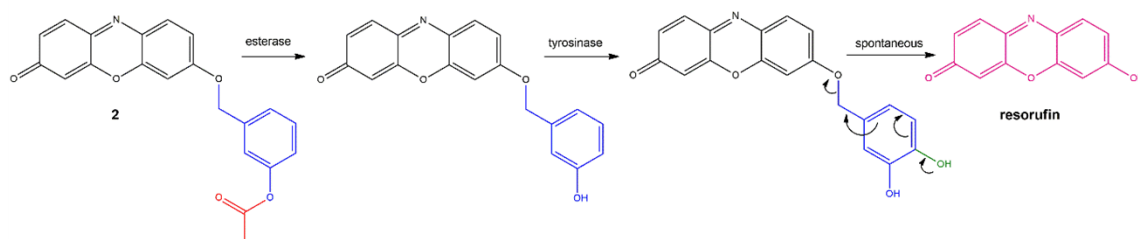
Scheme 1. Mechanism of fluorescent resorufin generation from compound 2 in the presence of esterase and tyrosinase enzymes. The presence of ester (red) prevents recognition of the ligand by tyrosinase. Removal of this group exposes tyrosinase binding site, leading to oxidation (green). Oxidized ligand spontaneously dissociate by 1,6-elimination producing fluorescent resorufin.

is filtrated to remove sodium sulfate and the solvent was removed using a rotary evaporator. Light yellow oil is obtained as a product. Purification with silica column chromatography results in partial decomposition. For this reason, the crude product is used in the final reaction without further purification (100 mg, 88% yield).

^{1}H NMR (400 MHz, CDCl$_3$, ppm) δ 7.37 (t, J = 7.8 Hz, 1H), 7.26 (m, 1H), 7.14 (m, 1H), 7.08-6.99 (m, 1H), 4.57 (s, 2H), 2.30 (s, 3H).

^{13}C NMR (400 MHz, CDCl$_3$, ppm) δ 169.61, 151.02, 139.24, 129.96, 126.14, 121.99, 121.85, 45.71, 21.36.

HRMS (ESI): Theoritical m/z for (M+Na)$^+$ is 250.9684 and experimental m/z for (M+Na)$^+$ is 250.18276.

2.1.2. 3-(((3-oxo-3H-phenoxazin-7-yl)oxy)methyl)phenyl acetate (2)

3-(bromomethyl)phenyl acetate (91 mg, 0.40 mmol) and resorufin sodium salt (70 mg, 0.30 mmol) were dissolved in 5 mL dimethylformamide (DMF). Potassium carbonate (138 mg, 1 mmol) was added and the reaction mixture was stirred for 16 h at 50 °C (Scheme 3). The crude product was extracted with dichloromethane and water. The organic layer is collected and dried using sodium sulfate. The solvent was removed using a rotary evaporator. The crude reaction mixture is purified with silica column chromatography using dichloromethane as mobile phase and solid orange product (2) was obtained (60 mg, 55% yield).

^{1}H NMR (400 MHz, DMSO-d_6, ppm) δ 7.80 (d, J = 8.6 Hz, 1H), 7.54 (d, J = 9.4 Hz, 1H), 7.46 (dd, J = 8.3, 4.1 Hz, 1H), 7.38 (d, J = 7.8 Hz, 1H), 7.26 (s, 1H), 7.21 (s, 1H), 7.17 – 7.06 (m, 2H), 6.79 (d, J = 9.5 Hz, 1H), 6.28 (d, J = 3.1 Hz, 1H), 5.30 (s, 2H), 2.28 (s, 3H).

^{13}C NMR (400 MHz, DMSO-d_6, ppm) δ 185.82, 169.68, 162.61, 151.09, 150.19, 145.83, 145.69, 138.21, 135.41, 134.25, 131.83, 130.19, 128.53, 125.71, 122.17, 121.63, 114.76, 106.14, 101.69, 70.13, 21.34.

2.2. Analysis of enzyme-responsiveness

In order to understand enzyme responsiveness of compound 2, 5 mM stock solution was prepared in dimethyl sulfoxide (DMSO). A second solution in PBS buffer (pH 7.4) was prepared with the final concentration of 20 μM. By using the latter solution compound 2 was either incubated alone, in the presence of esterase enzyme, in the presence of tyrosinase enzyme or in the presence of both enzymes for 120 min at 37 °C. Fluorescence spectra were recorded at 30 min intervals using the excitation wavelength of 550 nm. The final concentration of esterase (Esterase Porcine Liver, Enzyme Commission Number 3.1.1.1) and tyrosinase (Mushroom, Enzyme Commission Number 1.14.18.1) enzymes were 2.5 U/mL and 25 U/mL, respectively. In order to allow entry of fresh air, a needle was placed on the lids of reaction vials.

3. Results and discussion

Compound 2 was synthesised in two successive steps and obtained as orange solid with good yields. The compound was characterised using ^{1}H NMR, ^{13}C NMR, and high-resolution mass spectrometry. Consistent with literature data, O-functionalized resorufin displays a lower absorption at 478 nm and no fluorescence whereas resorufin absorbs at 571 nm and has bright fluorescence at 584 nm in phosphate saline buffer (PBS), at pH 7.4 (Figure 1). The quantum yield and extinction coefficient of the compound were calculated to be 0.04 and 5800 M^{-1}cm^{-1} respectively in PBS buffer. Compound 2 has a fluorescence quantum yield much lower than the tabulated value of resorufin (0.97 in water) consistent with the value of similar O-functionalized resorufin derivatives in literature [34, 44].

To assess the enzyme responsiveness of the probe, compound 2 is incubated alone or with various combinations of inputs and fluorescence spectra are analysed (Figure 2). Almost 70 fold enhancement in fluorescence at 584 nm is
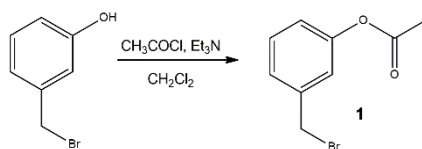
Scheme 2. Synthesis of compound 1.
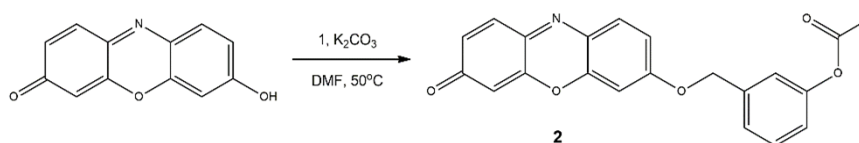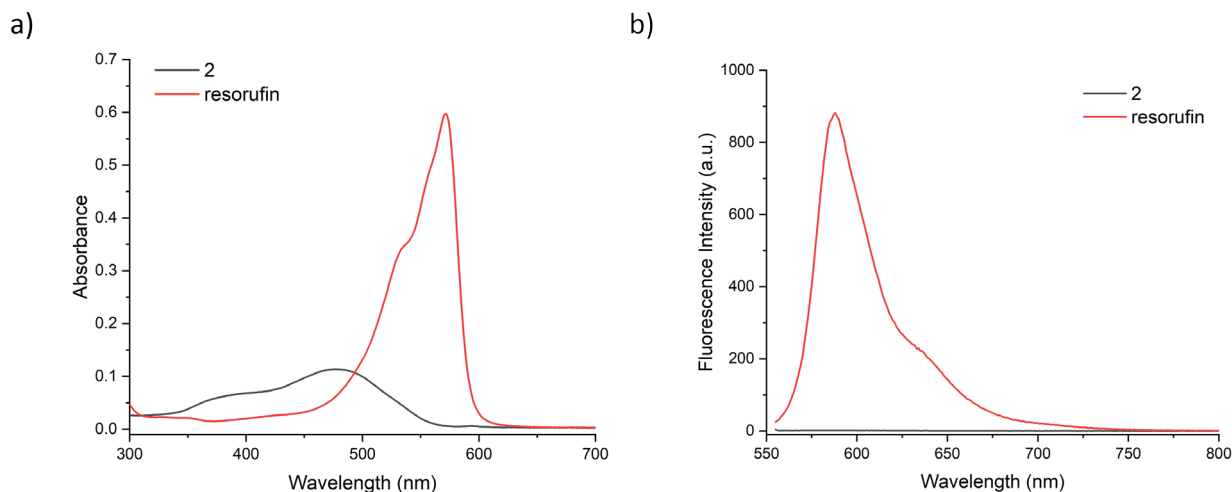

Scheme 3. Synthesis of compound 2.

Figure 1. UV-vis absorbance (a) and fluorescence spectra of 20 μM compound 2 (black) and resorufin (red) in PBS buffer, at pH 7.4. Fluorescence spectra are obtained by exciting the sample at 550 nm.
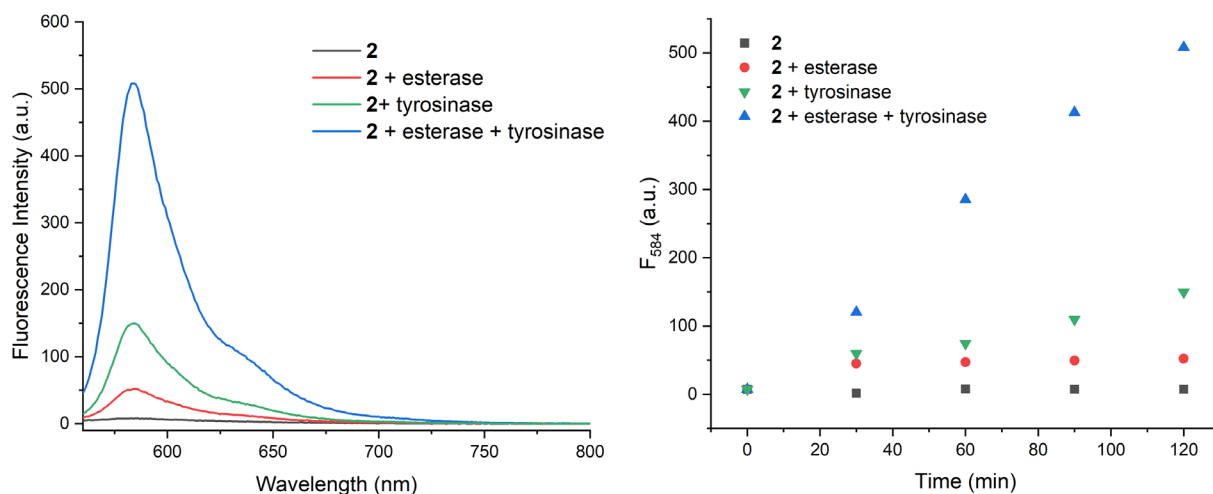

Figure 2. Fluorescence spectra of compound 2, 120 min after incubation with various input combinations (a) and time-dependent change in fluorescence intensity at 584 nm (b). Compound 2 (20 μM, in PBS, pH 7.4) is incubated at 37 °C either alone, with esterase (2.5 U/mL), with tyrosinase (25 U/mL), or with both enzymes for 120 min. Fluorescence at 584 nm is followed to analyse the formation of resorufin. Spectra are recorded by excitation at 550 nm.

detected when both esterase and tyrosinase enzymes are present in the solution. This value is significantly higher than the other input combinations (no enzymes, only esterase or only tyrosinase). Data suggest that in order to obtain fluorescent resorufin, activities of both enzymes are required. A moderate increase in tyrosinase applied samples may indicate slow spontaneous hydrolysis of ester bond in solution. With a separate more concentrated sample (100 μM in PBS buffer), the reaction is repeated with 100 U/mL tyrosinase and 2.5 U/mL esterase enzymes. Change in the solution colour and pink fluorescence of the enzyme-treated sample can be seen with naked eye (Figure S1a and S1b). Low-resolution mass analysis of the dual enzyme treated sample with LCMS proves the formation of resorufin peaks located at 212, corresponding to deprotonated product (Figure S1-c).

Dual enzyme-treated samples display an increase in the absorption above 550 nm, where free resorufin absorbs (Figure 3). This finding further proves the hypothesis depicted in Scheme 1. Results shown in Figure 2 suggest that when acyl bearing compound 2 is treated with tyrosinase only, fluorescence enhancement is very small. A structurally similar probe

that lacks acyl moiety on the structure is reported to be responsive to tyrosinase enzyme [34]. Hence, acyl derivatization seems to prevent enzyme catalysed conversion. To assess this further, Michaelis constant of the enzyme catalysed reaction is calculated. Solutions with different concentrations of compound 2 are treated with 3 U/mL of tyrosinase enzyme and the rate of fluorescence change is determined. Michaelis constant (K_m) is calculated to be 44.3 µM from the Lineweaver-Burke plot, which is approximately 1.5 fold higher than the tabulated value for a similar probe having ester-free 3-hydroxy phenyl ligand (Figure S2) [34]. This result indicates a lower affinity of the molecule to the enzyme when hydroxyl group is protected by an acyl group. Hence esterase is necessary for the removal of this group to be recognized by tyrosinase. From the same calculations, V_{max} is determined to be 0.37 µM.min^{-1}. When probe is incubated in the presence of an abundant serum protein (bovine serum albumin), reducing agents of the body (glutathione, ascorbate) or reactive oxygen species (hydrogen peroxide, hydroperoxide, and superoxide) there is no significant increase in fluorescence indicating the selectivity of the probe towards chosen enzymes (Figure S3).

Considering the data presented so far, compound 2 is shown to display a significant fluorescence enhancement upon incubation with both tyrosinase and esterase enzymes. When the enzymes are introduced alone, the increase is not significant. Altogether, the behaviour of the probe is like an AND logic operation as depicted in Figure 4a,4b. digitalized data is used to construct the truth table of the logic gate (Figure 4b). For the absence of the enzymes, '0' is written and for the presence of the enzymes '1' is written in the first two columns of the truth table. The last column of the table gives the output (fluorescence at 584 nm) and the value is assigned to be '1' if and only if the change in fluorescence is above 150 under experimental conditions. Therefore, the output can only be observed if both enzymes are present in the solution (both inputs are 1).

4. Conclusion

Fluorescent molecular sensors are very reliable and sensitive tools for diagnostic applications. Based on the design, sensors can selectively discriminate analytes including enzymes. Expression level and activities of enzymes differ with the progress of certain diseases and this change is usually used for the diagnosis. Since the change in the enzyme level and/or activity is tissue-specific, there should be more than one diagnostic enzyme data, for the accuracy of the analysis. Monitoring more than one disease marker would improve the reliability of the data. In the research presented here, a simple resorufin-based molecular structure is used to overcome this issue. In order to obtain a bright fluorescence, the presence of two enzymes is necessary. This property of the compound makes the molecule an information processing device, with a capacity to detect the signal and produces a readable output as a response. Relatively simple synthetic steps and the efficiency of the
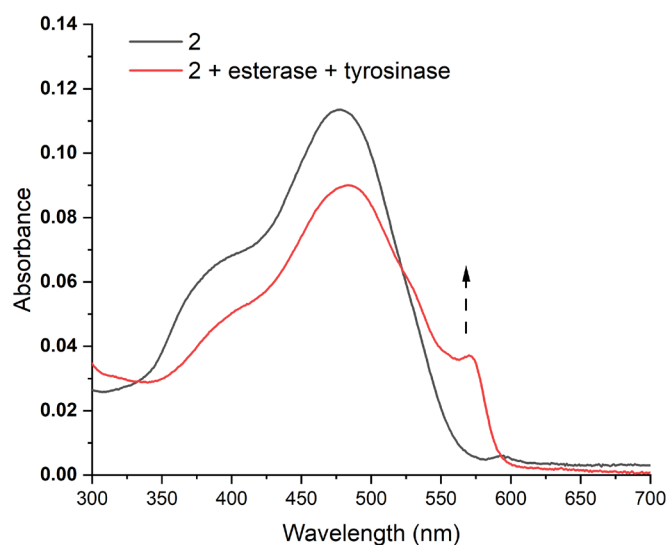

Figure 3. Change in UV-vis absorbance spectra of compound 2 (20 µM, PBS, pH 7.4) in the presence and absence of enzymes. Compound 2 is incubated with 2.5 U/mL esterase and 25 U/mL tyrosinase for 120 min at 37 °C. Peak above 550 nm appears in dual enzyme treated sample, consistent with the formation of resorufin (arrow).

a)

esterase
tyrosinase

AND → *hv*

b)

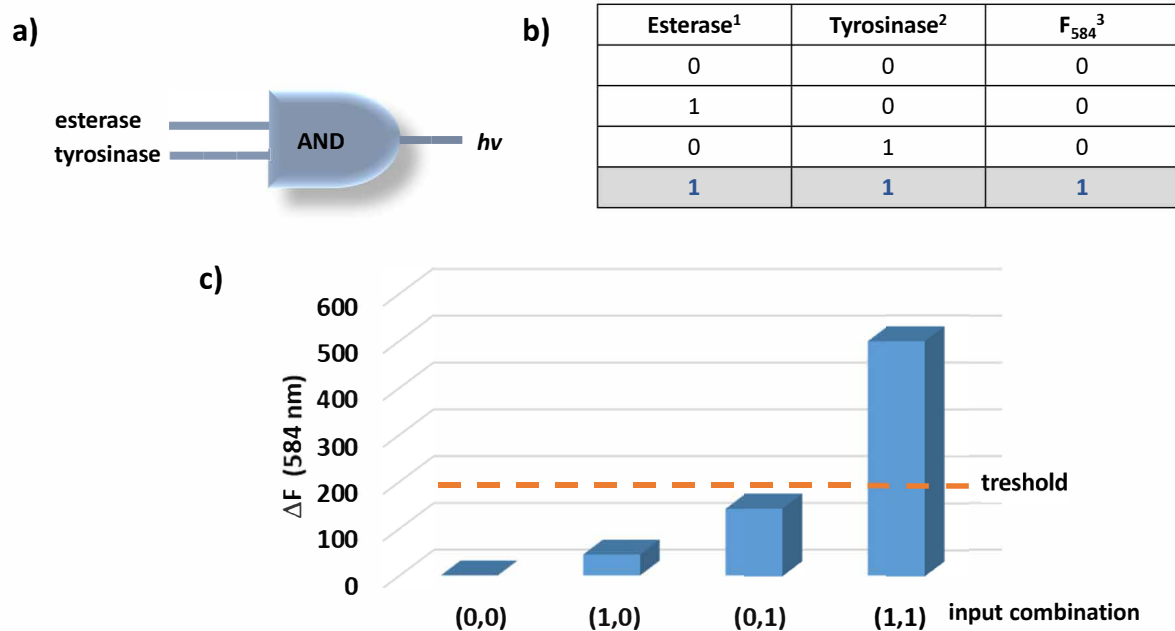| Esterase[1]	Tyrosinase[2]	F_{584}[3]
0	0	0
1	0	0
0	1	0
1	**1**	**1**

c)

Figure 4. AND logic gate diagram (a) and truth table (b). Threshold for the change in fluorescence is shown with orange dashed line (c). [1]esterase enzyme is used in 2.5 U/mL concentration. [2]Tyrosinase enzyme is used in 25 U/mL concentration. [3]Threshold for fluorescence change is taken to be 150 and the values beyond this value are accepted as 1 in the output column of the truth table.

enzymatic conversion makes this compound a good candidate for future applications in relevant biomedical areas such as in the diagnosis of drug-resistant melanomas. The same design strategy, hiding the enzyme binding site and exposing it with another analyte, can be used to make other enzyme responsive sensors. This may lead to the production of a library of sensors discriminating various diseases with different enzyme combinations. As conclusion, the dual enzyme responsive molecular logic gate presented here can be further modified to have useful applications in the future.

Acknowledgments

References

1. Liu M, Li C. Recent advances in actavatable organic photosensitizers for specific photodynamic therapy. ChemPlusChem 2020; 85 (5): 948-957. doi: 10.1002/cplu.202000203

2. Suzuki Y, Yokoyama K. Development of functional fluorescent molecular probes for the detection of biological substances. Biosensors 2015; 5 (2): 337-363. doi: 10.3390/bios5020337

3. Budyka, MF. Molecular switches and logic gates for information processing, the bottom-up strategy: from silicon to carbon, from molecules to supermolecules. Russian Chemical Reviews 2017; 86 (3): 181-210. doi: 10.1070/RCR4657

4. De Silva AP, Gunaratne HQN, McCoy CP. A molecular photoionic AND gate based on fluorescent signalling. Nature 1993; 364: 42-44. doi: 10.1038/364042a0

5. Erbas-Cakmak S, Kolemen S, Sedgwick AC, Gunnlaugsson T, James TD et. al. Molecular logic gates: The past, present and future. Chemical Society Reviews 2018; 47: 2228-2248. doi: 10.1039/C7CS00491E

6. Turkoglu G, Kayadibi Koygun G, Yurt MNZ, Pirencioglu S, Erbas-Cakmak S. A Therapeutic keypad lock decoded in drug resistant cancer cells. Chemical Science 2021; 12: 9754-9758. doi: 10.1039/D1SC02521J

7. Erbas Cakmak S, Bozdemir OA, Cakmak Y, Akkaya EU. Proof of Principle for a molecular 1:2 demultiplexer to function as an autonomously switching theranostic Device. Chemical Science 2013; 4: 858-862. doi: 10.1039/C2SC21499G

8.   Tregubov AA, Nikitin AA, Nikitin MP. Advanced smart nanomaterials with integrated logic-gating and biocomputing: Dawn of theranostic nanorobots. Chemical Reviews 2018; 118 (20): 10294-10348. doi: 10.1021/acs.chemrev.8b00198

9.   Turan IS, Gunaydın G, Ayan S, Akkaya EU. Molecular demultiplexer as a terminator automaton. Nature Communications 2018; 9: 805. doi: 10.1038/s41467-018-03259-z

10. Erbas-Cakmak,S, Pir Cakmak F, Demirel Topel S, Uyar TB, Akkaya EU. Selective photosensitization through an AND logic response: Optimization of the pH and glutathione response of activatable photosensitizers. Chemical Communication 2015; 51: 12258-12261. doi: 10.1039/C5CC01261A

11. Hettie KS, Klockow JL, Glass TE. Three-input logic gates with potential applications for neuronal imaging. Journal of American Chemical Society 2014; 136 (13): 4877-4880. doi: 10.1021/ja501211v

12. Rout B, Unger L, Armony G, Iron MA, Margulies D. Medication detection by a combinatorial fluorescent molecular sensor. Angewandte Chemie International Edition 2012; 51 (50): 12477-12481. doi: 10.1002/anie.201206374

13. Erbas-Cakmak S, Akkaya EU. Cascading molecular logic gates for advanced functions: A self-reporting, activatable photosensitizer", Angewandte Chemie International Edition 2013; 52 (43): 11364-11368. doi: 10.1002/anie.201306177

14. Upendar Reddy G, Axthelm J, Hoffmann P, Taye N, Glaser S et al. Co-registered molecular logic gate with a CO-releasing molecule triggered by light and peroxide. Journal of American Chemical Society 2017; 139 (14): 4991-4994. doi: 10.1021/jacs.7b00867

15. Ozlem S, Akkaya EU. Thinking outside the silicon box: Molecular AND logic as an additional layer of selectivity in singlet oxygen generation for photodynamic therapy. Journal of American Chemical Society 2009; 131 (1): 48-49. doi: 10.1021/ja808389t

16. Amir RJ, Ropkov M, Lerner RA, Barbas CF, Shabat D. Prodrug activation gated by a molecular "OR" logic trigger. Angewandte Chemie International Edition 2005; 44 (28): 4378-4381. doi: 10.1002/anie.200500842

17. Hammarson M, Andersson J, Li SM, Lincoln P, Andreasson J. Molecular AND-logic for dually controlled activation of a DNA-binding spiropyran. Chemical Communications 2010; 46: 7130-7132. doi: 10.1039/C0CC01682A

18. Sedgwick AC, Han HH, Gardiner JE, Bull SD, He XP et. al. The development of a novel AND logic based fluorescence probe for the detection of peroxynitrile and GSH. Chemical Science 2018; 9: 3672-3676. doi: 10.1039/C8SC00733K

19. de Luis B, García-Fernández A, Llopis-Lorente A, Villalonga R, Sancenón F et. al. A 1-to-2 demultiplexer hybrid nanocarrier for cargo delivery and activation. Chemical Communications 2020; 56: 9974-9977. doi:10.1039/D0CC03803B

20. Unger-Angel L, Motiei L, Margulies D. Molecular logic as a means to assess therapeutic antidotes. Frontiers in Chemistry 2019; 7: 243. doi: 10.3389/fchem.2019.00243

21. Deonarain MP, Epenetos AA. Targeting enzymes for cancer therapy: old enzymes in new roles. British Journal of Cancer 1994; 70 (5): 786-794. doi: 10.1038/bjc.1994.400

22. Singh H, Tiwari K, Tiwari R, Pramanik SK, Das A. Small molecule as fluorescent probes for monitoring intracellular enzymatic transformations. Chemical Reviews 2019; 119 (22): 11718-11760. doi: 10.1021/acs.chemrev.9b00379

23. Rajapaksha AA, Fu YX, Guo WY, Liu SY, Li ZW et. al. Review on the recent progress in the development of fluorescent probes targeting enzymes. Methods and Applications in Fluorescence 2021; 9 (3): 032001. doi: 10.1088/2050-6120/abf988

24. Dezso Z, Nikolsky Y, Sviridov E, Shi W, Serebriyskaya T et. al. A comprehensive functional analysis of tissue specificity of human gene expression. BMC Biology 2008; 6: 49. doi: 10.1186/1741-7007-6-49

25. Prost M, Hasserodt J. "Double gating" – a concept for enzyme-responsive imaging probes aiming at high tissue specificity. Chemical Communications 2014; 50: 14896–14899. doi: 10.1039/C4CC07147F

26. Kolanowski JL, Liu F, New EJ. Fluorescent probes for the simultaneous detection of multiple analytes in biology, Chemical Society Reviews 2018; 47: 195-208. doi: 10.1039/C7CS00528H.

27. Xie J, Mu R, Fang M, Cheng Y, Senchyna F et. al. A dual-caged resorufin probe for rapid screening of infections resistant to lactam antibiotics. Chemical Science 2021; 12: 9153-9161. doi: 10.1039/d1sc01471d

28. Romieu A. "AND" luminescent "reactive" molecular logic gates: a gateway to multi-analyte bioimaging and biosensing. Organic and Biomolecular Chemistry 2015; 13: 1294-1306. doi: 10.1039/C4OB02076F

29. Grimm JB, Gruber TD, Ortiz G, Brown TA, Lavis LD. Virginia orange: A versatile, red-shifted fluorescein scaffold for single- and dual-input fluorogenic probes. Bioconjugate Chemistry 2016; 27 (2): 474-480. doi: 10.1021/acs.bioconjchem.5b00566

30. Li Y, Wang H, Li J, Zheng J, Xu X et. al. Simultaneous intracellular β-D-glucosidase and phosphodiesterase I activities measurements based on a triple-signaling fluorescent probe. Analytical Chemistry 2011; 83 (4): 1268-1274. doi: 10.1021/ac102095j

31. Chen Y. Advances in fluorescent probes for detection and imaging of endogenous tyrosinase activity. Analytical Biochemistry 2020; 594: 113614. doi: 10.1016/j.ab.2020.113614

32. Zhan C, Cheng J, Li B, Huang S, Zeng F et. al. A Fluorescent probe for early detection of melanoma and its metastasis by specifically imaging tyrosinase activity in a mouse model. Analytical Chemistry 2018; 90 (15): 8807-8815. doi: 10.1021/acs.analchem.8b00594.

33. Wu X, Li L, Shi W, Gong Q, Ma H. Near-infrared fluorescent probe with new recognition moiety for specific detection of tyrosinase activity: design, synthesis, and application in living cells and zebrafish. Angewandte Chemie International Edition 2016; 55 (47): 14728-14732. doi: 10.1002/anie.201609895

34. Wu X, Li X, Li H, Shi W, Ma H. A highly sensitive and selective fluorescent off-on probe for the detection of intracellular endogenous tyrosinase activity. Chemical Communications 2017; 53: 2443-2446. doi: 10.1039/C6CC09679D

35. La X, Wichers HJ, Soler-Lopez M, Dijkstra BW. Structure and function of human tyrosinase and tyrosinase-related proteins. Chemistry 2018; 24 (1): 47-55. doi: 10.1002/chem.201704410

36. Saran A, Spinola M, Pazzaglia S, Peissel B, Tiveron C et. al. Loss of tyrosinase activity confers increased skin tumor susceptibility in mice. Oncogene 2004; 23 (23): 4130-4135. doi: 10.1038/sj.onc.1207565

37. Hinz M, Stein A, Cole T. Parkinson's disease-associated melanin steal. Neuropsychiatric Disease and Treatment 2014; 10: 2331-2337. doi: 10.2147/NDT.S74952

38. Laizure SC, Herring V, Hu Z, Witbrodt K, Parker RB. The role of human carboxylesterases in drug metabolism: have we overlooked their importance? Pharmacotherapy 2013; 33 (2): 210-222. doi: 10.1002/phar.1194

39. Wang H, Su H, Wang N, Wang J, Zhang J et. al. Recent development of reactional small-molecule fluorescent probes based on resorufin. Dyes and Pigments 2021; 191: 109351. doi: 10.1016/j.dyepig.2021.109351

40. Tian L, Feng, H, Dai Z, Zhang R. Resorufin-based responsive probes for fluorescence and colorimetric analysis. Journal of Materials Chemistry B 2021; 9: 53-79. doi: 10.1039/D0TB01628D

41. Zhao L, Li X, Gao X, Zhang Y, Shi W et. al. Nitroreductase detection and hypoxic tumor cell imaging by a designed sensitive and selective fluorescent probe, 7-[(5-Nitrofuran-2-yl) methoxy]-3H-phenoxazin-3-one. Analytical Chemistry 2013; 85 (8): 3926-3932. doi: 10.1021/ac400750r

42. Gao W, Xing B, Tsien RY, Rao J. Novel fluorogenic substrates for imaging b-lactamase gene expression. Journal of American Chemical Society 2003; 125 (37): 11146-11147. doi: 10.1021/ja036126o

43. Albers AE, Rawls KA, Chang CJ. Activity-based fluorescent reporters for monoamine oxidases in living cells. Chemical Communications 2007; 4647-4649. doi: 10.1039/B713190A

44. Xu W, Kong JS, Yeh YTE, Chen P. Single-molecule nanocatalysis reveals heterogeneous reaction pathways and catalytic dynamics. Nature Materials 2008; 7: 992-996. doi:10.1038/nmat2319

Supporting Information

Development of Dual Enzyme Responsive Molecular AND Logic Gate

Sundus Erbas-Cakmak[1,2*]

[1]Department of Molecular Biology and Genetics, Konya Food and Agriculture University, Konya,

Turkey

[2]Biotechnology Graduate Program, Konya Food and Agriculture University, Konya, Turkey

Table of Contents

1. **General Information**

All reagents and solvents were purchased from commercial sources and used without further purification. Column chromatography was carried out using silica stationary phase (230–400 mesh, SiliCycle Inc., Canada). Analytical thin layer chromatography was performed on 0.25 mm thick precoated silica gel plates (60F254, Merck, Germany). Esterase enzyme is obtained from Sigma-Aldrich (Porcine Liver Esterase, Enzyme Commission Number 3.1.1.1) and tyrosinase enzyme was purchased from Sigma (mushroom tyrosinase, Enzyme Commision Number 1.14.18.1). Compounds were visualized under UV light. All ^{1}H NMR ad ^{13}C NMR spectra were recorded on a Varian Inova instrument (400 MHz) at Selçuk University and Ataturk University respectively. Chemical shifts (δ) are reported in parts per million (ppm) and referenced to the residual solvent peak. Coupling constants (J) are reported in hertz (Hz). Standard abbreviations indicating multiplicities are given: b = broad, d = doublet, m = multiplet, s = singlet, t = triplet. High-resolution mass spectrometry was carried out using Agilent 6530 Accurate-Mass Q-TOF LC/MS of the Eastern Anatolia Advanced Technology Research and Application Centre (DAYTAM, Erzurum, Turkey). UV-Vis Absorbance and Fluorescence Spectrometry (Agilent, Varian) of Konya Food and Agriculture University are used for spectroscopic analysis. LC-MS data were recorded using Schimadzu LCMS-2020 Single Quadrupole Liquid Chromatography Mass Spectrometer located at Konya Food and Agriculture University.

2. Additional Experimental Procedures

2.1. Calculation of Quantum yield and Extinction Coefficient

Absorbance and Fluorescence spectra of compounds and reference sample were recorded in PBS buffer and water respectively. As the reference compound Rhodamine 6G is used. Tabulated quantum yield of this compound is used in calculations (0.97 in water)[1] using the Formula 1 given below.[2] Samples are excited at 488 nm.

$$Q = Q_R \, (I/I_R)*(A_R/A)*(n^2/n_R^2) \qquad \text{(Formula 1)}$$

Integrated areas of fluorescence for sample and reference compound (I and I_R respectively) are calculated using Origin software. A and A_R are absorbance values at 488 nm for sample and reference compound respectively. n is the refractive index and this value is taken to be 1.333, corresponding to the value for water. Quantum yield of Rhodamine 6G (Q_R) is taken to be 0.95.

Extinction coefficient is determined using Beer-Lambert formula (Formula 2), taking the length of light path (l) as 1 cm.

$$A = \varepsilon\, C\, l \qquad \text{(Formula 2)}$$

In the Formula 2, C refers to concentration of the sample in PBS buffer, A is the absorbance and ε is the extinction coefficient.

2.2. Determination of Michaelis Constant and Maximum Rates

Samples containing 10, 20, 30, 40 and 50 μM of compound **2** in the presence of 3U/ml tyrosinase enzyme in PBS buffer (pH 7.4) were incubated at 37°C and fluorescence spectra were recorded. Fluorescence was recorded at 0, 15, 45 and 75 minutes. From the time dependent fluorescence change of the samples, initial rates of reactions were calculated for each sample. The data is plotted as Lineweaver-Burke plot as shown in Figure S2. Linear fitting of the data points gives the equation 1 below. Using the slope and intercept values of the equation, Michaelis constant (K_m) and maximum rate of enzymatic conversion (V_{max}) were calculated. [S] in the equation represents the concentration of compound **2**.

$$1/V_0 = (K_m/V_{max})*(1/[S]) + 1/V_{max} \qquad \text{(Equation 1)}$$

2.3. Selectivity Experiment

Compound **2** (20 μM) was prepared in PBS buffer (pH 7.4). Various analytes were added at the concentrations relevant to physiological ones and incubated for 120 min at 37°C. Fluorescence spectra were recorded and compared with the spectra of dual enzyme treated Compound **2** as shown in Figure S3. Concentrations of the analytes were 1 mM for glutathione (GSH) and sodium ascorbate, 100 μM for Bovine Serum Albumin (BSA), tert-butyl hydroperoxide (TBHP), hydrogen peroxide, potassium superoxide and finally 25U/ml for tyrosinase and 2.5U/ml for esterase.

3. Additional Figures

In order to understand the colour and fluorescence change more obviously with naked eye and by Mass Spectrometry analysis, more concentrated compound **2** was prepared (100 μM in PBS buffer). To this solution, esterase enzyme (2.5 U/ml) and tyrosinase enzyme (100 U/ml) were added. A photo under day light and UV light is taken (Figure S1-a and S1-b respectively). Colour change and generation of bright pink fluorescence is clearly seen in dual enzyme treated samples. LC-MS analysis from enzyme treated samples proves the formation of resorufin with a peak value at 212 corresponding to $(M-H)^-$.
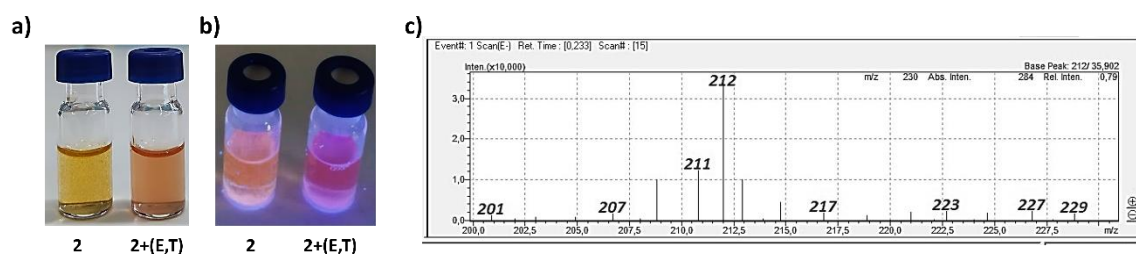
Figure S1. Compound **2** (100 μM) in PBS buffer (pH 7.4) under daylight (a) and under UV light (b). Compound **2** is incubated with esterase (2.5 U/ml) and tyrosinase (100 U/ml) enzymes for 30 min in right samples of each photo. Low resolution mass spectra obtained by LCMS analysis of enzyme treated sample (c) proves the formation of resorufin with m/z of 212 corresponding to $(M-H)^-$.

To determine the Michaelis constant of tyrosinase enzyme, substrate dependency of rates are plotted in the form of Lineweaver-Burke plot (Figure S2). From the slope and intercept values K_m and V_{max} are calculated as described in previous section.
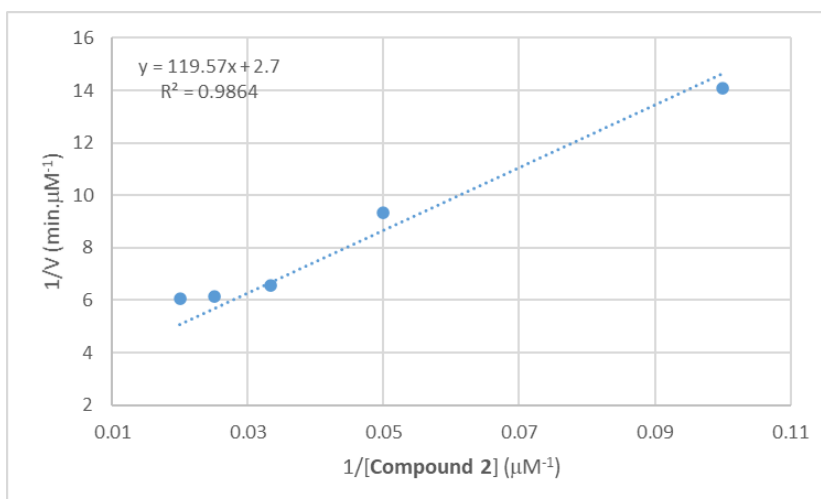
Figure S2. Lineweaver-Burke plot for conversion rate of compound **2** (10-50 μM) in the presence of 3 U/ml tyrosinase enzyme in PBS buffer, at 37°C.
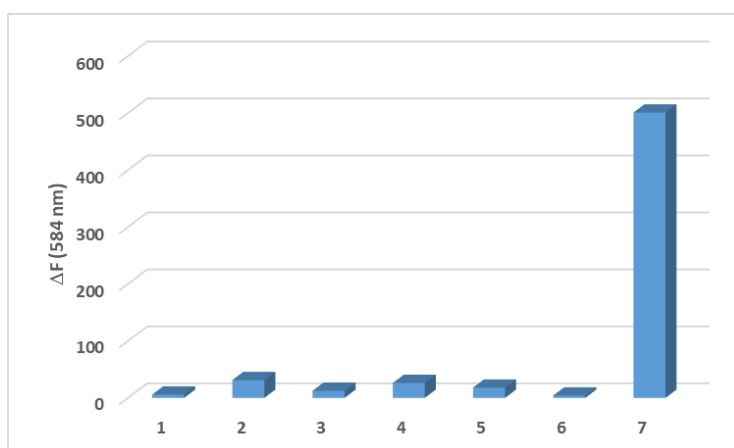

Figure S3. Selectivity of the compound **2** towards various different analytes. Samples contains (1) 100 μM BSA; (2) 1mM GSH; (3) 1 mM sodium ascorbate; (4) 100 μM H_2O_2; (5) 100 μM KO_2; (6) 100 μM TBHP; (7) 25U/ml tyrosinase and 2.5U/ml esterase enzymes. Excitation wavelength is 550 nm.
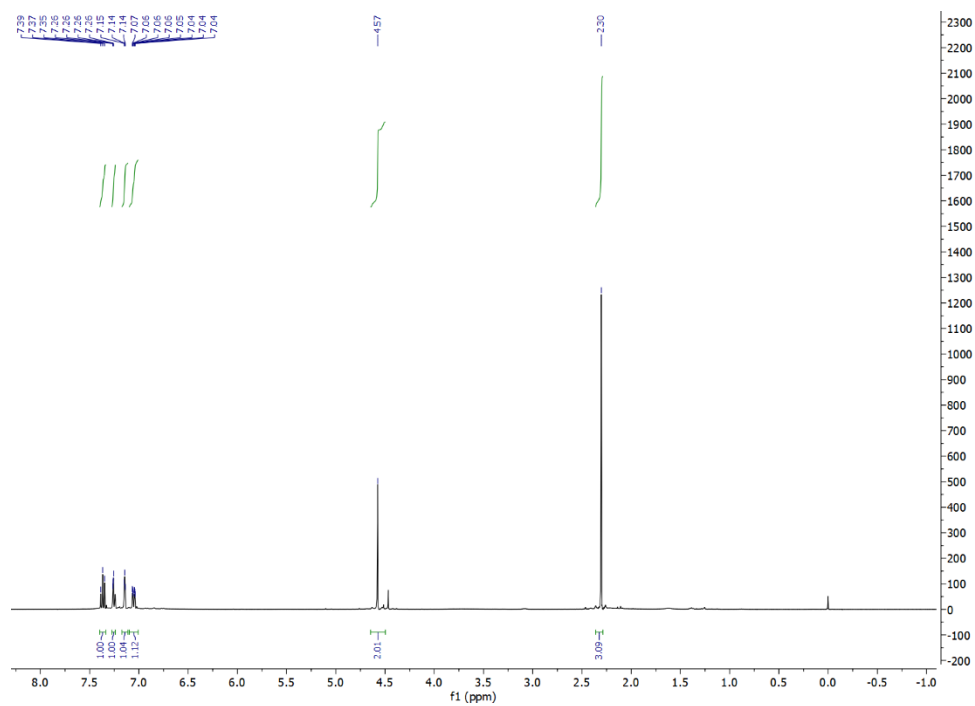
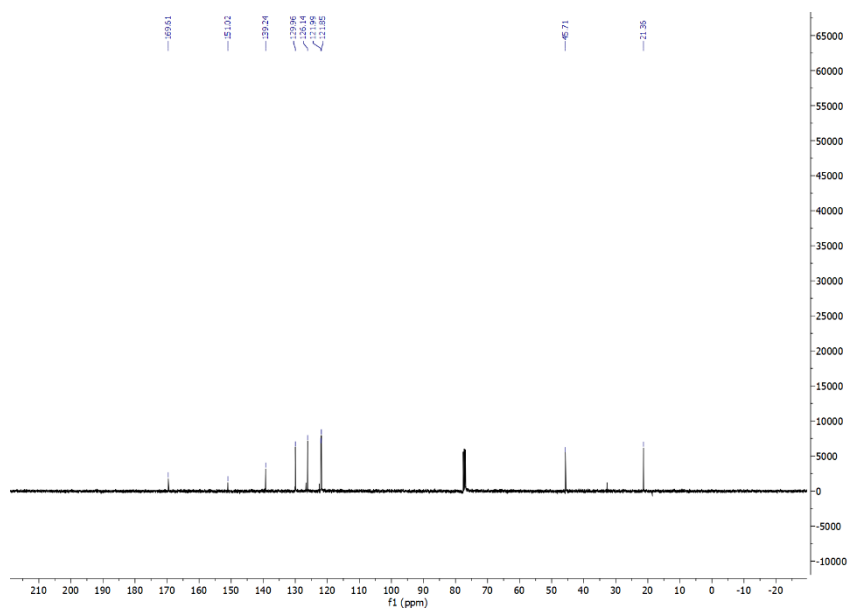Figure S4. ^{1}H NMR spectrum of compound **1** (400 MHz, CDCl$_3$)

Figure S5. ^{13}C NMR spectrum of compound **1** (400 MHz, CDCl$_3$)

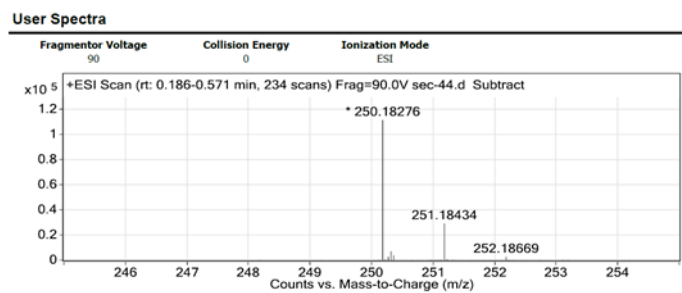| Fragmentor Voltage	Collision Energy	Ionization Mode
90	0	ESI

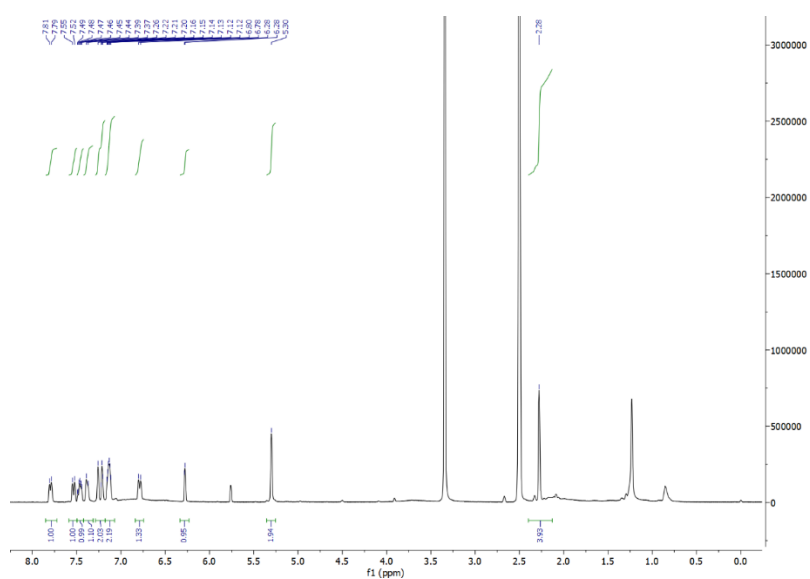Figure S6. HRMS (ESI) spectrum of compound **1**

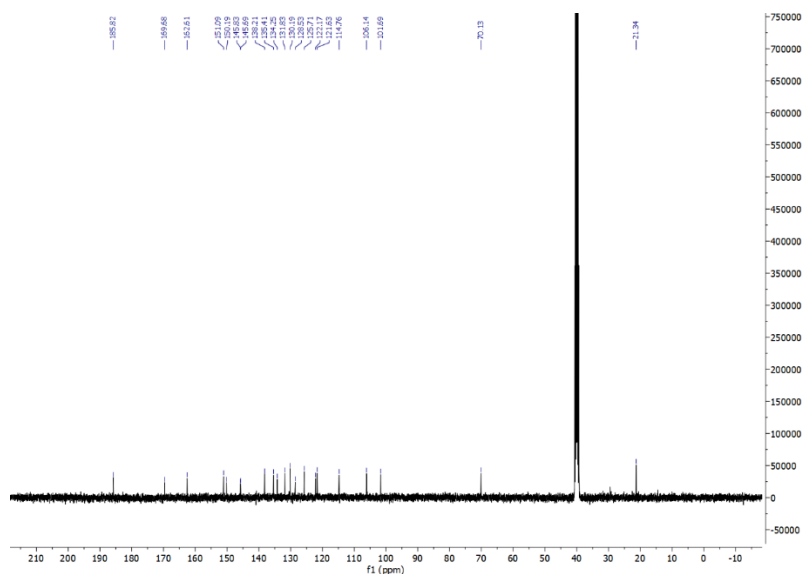Figure S7. ^{1}H NMR spectrum of compound **2** (400 MHz, DMSO-d_6)

Figure S8. ^{13}C NMR spectrum of compound **2** (400 MHz, DMSO-d_6)

4. References

1. Bozdemir OA, Erbas-Cakmak S, Ekiz OO, Dana A, Akkaya EU. Towards Unimolecular Luminescent Solar Concentrators: Bodipy-Based Dendritic Energy Transfer Cascade with Panchromatic Absorption and Monochromatized Emission", Bozdemir, O. A., Erbas-Cakmak, S., Ekiz, O. Ö., Dana, A., Akkaya, E. U., 2011, Angewandte Chemie International Edition 2011, 50: 10907-10912. Doi: 10.1002/anie.201104846

2. Xu W, Kong JS, Yeh YTE, Chen P. Single-molecule nanocatalysis reveals heterogeneous reaction pathways and catalytic dynamics. Nature Materials 2008; 7: 992-996. doi: 10.1038/nmat2319